Distinctive nuclear organisation of centromeres and regions involved in pluripotency in human embryonic stem cells

Anne E. Wiblin[1], Wei Cui[2], A. John Clark[2] and Wendy A. Bickmore[1,*]

[1]MRC Human Genetics Unit, Crewe Road, Edinburgh, EH4 2XU, UK
[2]Roslin Institute, Roslin BioCentre, Midlothian, EH25 9PS, UK
*Author for correspondence (e-mail: w.bickmore@hgu.mrc.ac.uk)

Accepted 13 May 2005
Journal of Cell Science 118, 3861-3868 Published by The Company of Biologists 2005
doi:10.1242/jcs.02500

Summary

Nuclear organisation is thought to be important in regulating gene expression. Here we investigate whether human embryonic stem cells (hES) have a particular nuclear organisation, which could be important for maintaining their pluripotent state. We found that whereas the nuclei of hES cells have a general gene-density-related radial organisation of chromosomes, as is seen in differentiated cells, there are also distinctive localisations for chromosome regions and gene loci with a role in pluripotency. Chromosome 12p, a region of the human genome that contains clustered pluripotency genes including *NANOG*, has a more central nuclear localisation in ES cells than in differentiated cells. On chromosome 6p we find no overall change in nuclear chromosome position, but instead we detect a relocalisation of the *OCT4* locus, to a position outside its chromosome territory. There is also a smaller proportion of centromeres located close to the nuclear periphery in hES cells compared to differentiated cells. We conclude that hES cell nuclei have a distinct nuclear architecture, especially at loci involved in maintaining pluripotency. Understanding this level of hES cell biology provides a framework within which other large-scale chromatin changes that may accompany differentiation can be considered.

Key words: Centromere, Chromosome territory, Embryonic stem cell, *NANOG*, Nucleus, *OCT4*

Introduction

The human genome is spatially organised within the nuclei of differentiated cells. There is a radial arrangement of chromosome territories (CTs): gene-rich chromosomes such as chromosome 19 (HSA19) concentrate in the centre of the nucleus and more gene-poor chromosomes (e.g. chromosome 18) localise toward the nuclear periphery (Croft et al., 1999; Boyle et al., 2001; Cremer et al., 2001; Cremer et al., 2003). Centromeres are also generally found at the nuclear periphery, or around nucleoli (Carvalho et al., 2001; Weierich et al., 2003; Gilchrist et al., 2004), whereas telomeres are mainly found in the nuclear interior (Weierich et al., 2003). Gene clusters, and individual chromosomal domains also have distinctive localisations within respect to their CTs (Volpi et al., 2000; Williams et al., 2002; Mahy et al., 2002a).

In model organisms it is clear that nuclear organisation can regulate gene expression (Spector, 2003). Data are consistent with nuclear organisation also being a determinant of gene expression for the human genome. Therefore, there may be differences in the nuclear organisation of different cell types. Indeed, in some human cell types (amniocytes and fibroblasts) with flat/ellipsoid-shaped nuclei, HSA18 can be found toward the nuclear centre rather than at the nuclear periphery, as is typical in cells with more spherical nuclei (lymphocytes, keratinocytes, colon and cervix epithelial cells) (Cremer et al., 2001; Cremer et al., 2003). In the mouse, differences in the spatial and radial distribution of chromosomes have been documented in different tissues of the animal (Parada et al., 2004) as well as during the differentiation of T cells (Kim et al., 2004). However, to date no significant change in radial position of a human chromosome within the nucleus has been documented during differentiation, although there may be changes in chromosome associations (Kuroda et al., 2004).

Within CTs themselves, the position of gene clusters is altered in different differentiated human cell types (Volpi et al., 2000; Williams et al., 2002). This aspect of nuclear organisation has not been studied in human stem cells, but in the mouse, movement of specific genes out of CTs has been seen upon the differentiation of ES cells (Chambeyron and Bickmore, 2004). Human centromeres are localised close to either the nuclear periphery or the nucleolus (Carvalho et al., 2001; Weierich et al., 2003). However, changes of centromere distribution in relation to cell cycle, physiological or differentiation state have been reported (reviewed by Gilchrist et al., 2004). In addition, lineage-specific centromere associations into chromocentres have been reported during lymphoid and myeloid differentiation, with an overall increase in centromere clustering towards later stages of differentiation (Beil et al., 2002; Alcobia et al., 2003).

If nuclear organisation regulates gene expression, then it may have a key role in restricting it, as cells become more committed to a differentiation pathway. Therefore it is

important to determine how the genome is organised in the nucleus of pluripotent cells, and particularly in stem cells (Fisher and Merkenschlager, 2002). The organisation of human chromosomes and centromeres has been studied in haemopoietic progenitor cells (Cremer et al., 2003) and in $CD34^+$ stem cells from umbilical cord blood (Alcobia et al., 2003). However, there have been no studies of nuclear organisation in hES cells.

Human ES cells have been derived from the inner cell mass of blastocysts, and as well as being able to self-renew, they have the ability to differentiate into all three embryonic germ layers when injected into severe combined immunodeficient mice (Thomson et al., 1998). It is anticipated that hES cells will be an important tool for understanding early human development, with the hope that they may also have therapeutic potential. Although they share many features with mouse ES (mES) cells, including the expression of common genes important for pluripotency, there are also key differences between mES and hES cells (Pera and Trounson, 2004; Ginis et al., 2004). Moreover, there are fundamental differences in the organisation of chromosomes between the human and mouse genomes. Therefore, mES cells cannot serve as a suitable model for studying the nuclear organisation of human stem cells and an investigation of hES cell nuclei is required.

Here we compared the nuclear organisation of differentiated human cells with hES cells. We show that hES cells have a radial organisation of chromosomes in the nucleus that relates to gene density and that is typical of many differentiated cell types. However, we find differences in the localisation of chromosomes and gene loci with known roles in pluripotency. We also describe differences in centromere position in hES cell nuclei.

Materials and Methods

Human ES cell culture and analysis

Human ES cell lines H1 (46XY), H7 and H9 (46XX) (Thomson et al., 1998) were grown as previously described, with minor modification (Xu et al., 2001). Briefly, the cells were cultured on Matrigel-coated culture dishes with mouse embryonic fibroblast conditioned medium supplemented with 8 ng/ml basic fibroblast growth factor. Cells were routinely split 1:3 with collagenase. H7 cells were passage (p)55. H1 cells were used at p42-65 and H9 cells were at p39-55.

The cells were analysed by flow cytometry for the hES cell surface antigens SSEA4 and Tra-1-60 using a FACScan (BD Biosciences). Briefly, hES cells were harvested by trypsin/EDTA and washed with phosphate-buffered saline (PBS). After treatment with 10% goat serum to block non-specific binding, the cells were incubated with monoclonal antibodies against SSEA4 (1:5, DSHB, IA) or Tra-1-60 (1:12, Chemicon) on ice for 30 minutes. The cells were then treated with goat anti-mouse IgG3-FITC or goat anti-mouse IgM-PE (both at 1:100, Southern Biotechnologies). Finally, 10^4 cells were acquired for each sample and analysed with CELLQUEST software.

Human (46XY) 1HD primary fibroblasts and FATO LCLs (46XY) were grown as described previously (Croft et al., 1999).

Fluorescence in situ hybridisation

Chromosome paints were labelled with biotin-16-dUTP by nick translation or by PCR amplification (Croft et al., 1999) or obtained commercially (Cambio). BACs were labelled by nick translation with digoxigenin-11-dUTP. 200 ng paint and 70 ng BAC were used per slide, with 6 μg human Cot1 DNA (GIBCO BRL) as competitor.

For 2D analysis, cells were swollen in 75 mM KCl before fixation in 3:1 methanol:acetic acid. Hybridisation was as described previously (Croft et al., 1999) but with the denaturing time reduced to 1.15 minutes for hES cells. For 3D analysis, hES cells were trypsinised and washed twice in PBS before permeabilisation in CSK buffer (100 mM NaCl, 300 mM sucrose, 3 mM $MgCl_2$, 10 mM PIPES, pH 6.8, 0.5% Triton X-100) for 5 minutes on ice. After washing in PBS, cells were fixed with 4% paraformaldehyde/PBS for 10 minutes, washed again in PBS and cytospun onto slides at 11 ***g*** (Shandon, Cytospin3) for 5 minutes. Slides were then subjected to freeze-thaw in 20% glycerol/PBS and FISH was carried out as described previously (Croft et al., 1999). To check the preservation of nuclear structure after cytospinning, we compared the nuclear organisation of centromeres in primary fibroblasts grown on slides to that of primary fibroblasts cytospun onto slides.

After hybridisation, biotinylated probes were detected using fluorochrome-conjugated avidin (FITC or Texas Red) (Vector Laboratories) followed by biotinylated anti-avidin (Vector Laboratories) and a final layer of fluorochrome-conjugated avidin. Digoxigenin-labelled probes were detected with sequential layers of FITC-conjugated antidigoxigenin (BCL) and FITC-conjugated anti-sheep antibody (Vector Laboratories). Slides were counterstained with 0.5 μg/ml DAPI. Telomere FISH was carried out using a telomere PNA FISH Kit (DAKO).

Immunofluorescence

Centromeres were detected by immunofluorescence using either a CENP-C antibody (gift of W. Earnshaw, Wellcome Trust Centre for Cell Biology, University of Edinburgh, UK) and FITC-conjugated anti-rabbit secondary antibody, or CREST serum and a Texas Red anti-human secondary antibody. PML bodies were detected using 5S10 monoclonal antibody and Texas Red anti-mouse secondary antibody. Nucleoli were detected using a Ki67 antibody and FITC-conjugated anti-rabbit secondary antibody. All secondary antibodies were supplied by Jackson ImmunoResearch Laboratories.

Image capture and image analysis

2D slides were examined using a Zeiss Axioplan fluorescence microscope fitted with a triple band-pass filter (Chroma #83000). Grey-scale images were captured with a cooled CCD camera (Princeton Instruments Pentamax) and analysed using custom IPLab scripts. For 3D analysis, a focus motor was used to collect images at 0.25μm intervals in the *z*-plane using a Xillig CCD camera. 3D image stacks were analysed using IPLab and deconvolved using Hazebuster (Vaytek).

The radial distribution of CTs was determined in 2D specimens by an erosion script, as previously described (Croft et al., 1999). The radial distribution of specific gene loci was assessed manually across the five erosion shells from the edge (shell 1) to the centre (shell 5) of the nucleus. These distributions were normalised to the proportion of the total DAPI signal present in each shell. 3D chromosome position was determined as previously described (Bridger et al., 2000).

Analysis of probe position relative to the surface of CTs, and interphase separation (*d*) were as previously described (Mahy et al., 2002a; Mahy et al., 2002b; Chambeyron and Bickmore, 2004). Differences in the nuclear position of CTs and gene loci were tested for statistical significance using a Mann-Whitney U test in Minitab 13. This is a nonparametric test of the hypothesis that two groups come from the same distribution, without assuming that the data are normally distributed.

3D analysis of centromeres and telomeres in the *z*-plane was performed using a custom IPLab script. Briefly, the script defines the outline of the DAPI nucleus in each frame of the *z*-stack, calculates the highest level of intensity for each fluorescent spot and locates which frame the spot is positioned in.

Results

HSA18 and 19 have a radial distribution in the nuclei of human ES cells

The radial distribution of CTs in the nucleus, related to their gene density, was first described for HSA18 and 19 (Croft et al., 1999). These chromosomes are of approximately the same size (76 and 63 Mb, respectively) but HSA18 is very gene-poor, harbouring an estimated 449 genes, whereas HSA19 is very gene-rich with 1528 genes (http://www.ensembl.org/Homo_sapiens/). HSA18 is found towards the nuclear periphery in a variety of differentiated cells and HSA19 is in the centre of the nucleus (Croft et al., 1999; Cremer et al., 2003). This radial distribution is conserved amongst primates (Tanabe et al., 2002) and it is also applicable to other human chromosomes (Cremer et al., 2001; Boyle et al., 2001).

We investigated the radial position of HSA18 and HSA19 in the nuclei of H1 (XY) and H9 (XX) hES cells. The cells were cultured on Matrigel and the expression of cell-surface antigens SSEA-4 and Tra-1-60 cells was analysed by flow cytometry. Of the H1 cells, 70% were SSEA-4 positive and 55% were positive for Tra-I-60, indicating that most of the cells in the culture were undifferentiated (Draper et al., 2002; Carpenter et al., 2004). Chromosome position was first established using fluorescence in situ hybridisation (FISH) with chromosome paints for HSA18 and 19 in 2D preparations (Fig. 1A). Although this flattens nuclear morphology, it does not alter the measured radial distribution of chromosomes (Croft et al., 1999), and it allows for rapid and automated analysis of large numbers of nuclei. The radial position of each CT was established from the distribution of hybridisation signal, relative to that of total DNA, in five erosion shells (Croft et al., 1999; Boyle et al., 2001). In both cell lines, HSA19 has a more central nuclear location than HSA18 ($P \leqslant 0.001$), and data for H1 cells is shown in Fig. 1B. This was confirmed by 3D analysis of H1 cells (Fig. 1C). HSA18 is significantly closer to the nuclear periphery than HSA19 in the x and y-axes ($P \leqslant 0.001$), though differences through the z-axis were not significant ($P=0.68$).

An altered nuclear distribution of 12p in human ES cells

The data in Fig. 1 suggest that CTs in hES cell nuclei have a gene-density-related radial organisation similar to that seen in many differentiated human cell types. (Cremer et al., 2001; Cremer et al., 2003). To determine whether there might be changes in the nuclear distribution of specific CTs in hES cells, we examined the radial position of the CTs that carry genes with a known role in maintaining the undifferentiated state. *OCT4 (POU5F1)* is located within a cluster of non-class I genes embedded within the MHC class I region on HSA6p21.33. *OCT4* expression is essential to maintain the undifferentiated phenotype of hES cells (Matin et al., 2004). *NANOG* (12p13.31) expression is also required to maintain the undifferentiated state of hES cells (Zaehres et al., 2005). We hybridised chromosome paints for 6p and 12p, together with BACs for *OCT4* and *NANOG*, to nuclei from hES cells and lymphoblastoid cells (LCLs) (Fig. 2A). The radial position of the CTs was established using the same erosion analysis as used in Fig. 1. We have previously reported that human chromosomes 6 and 12 have nuclear distributions in LCLs and fibroblasts that are intermediate between those of HSA18 and HSA19, i.e. they are located neither at the nuclear periphery, nor in the nuclear centre (Boyle et al., 2001). This was confirmed here for 6p and 12p in LCLs (Fig. 2B). There was no significant difference in the radial position of 6p between LCLs and hES cells. However, 12p was located significantly closer to the nuclear centre (shell 5) in hES cells compared to LCLs ($P=0.04$) (Fig. 2B).

Nuclear organisation of pluripotency genes in ES and differentiated cells

If CT radial position differs between ES cells and differentiated cell types, then it might be expected that the radial position of specific gene loci on these chromosomes follow that of their host chromosome. Consistent with this, *NANOG* (12p), but not *OCT4* (6p) was located closer to the nuclear centre in hES compared with LCLs (Fig. 2C).

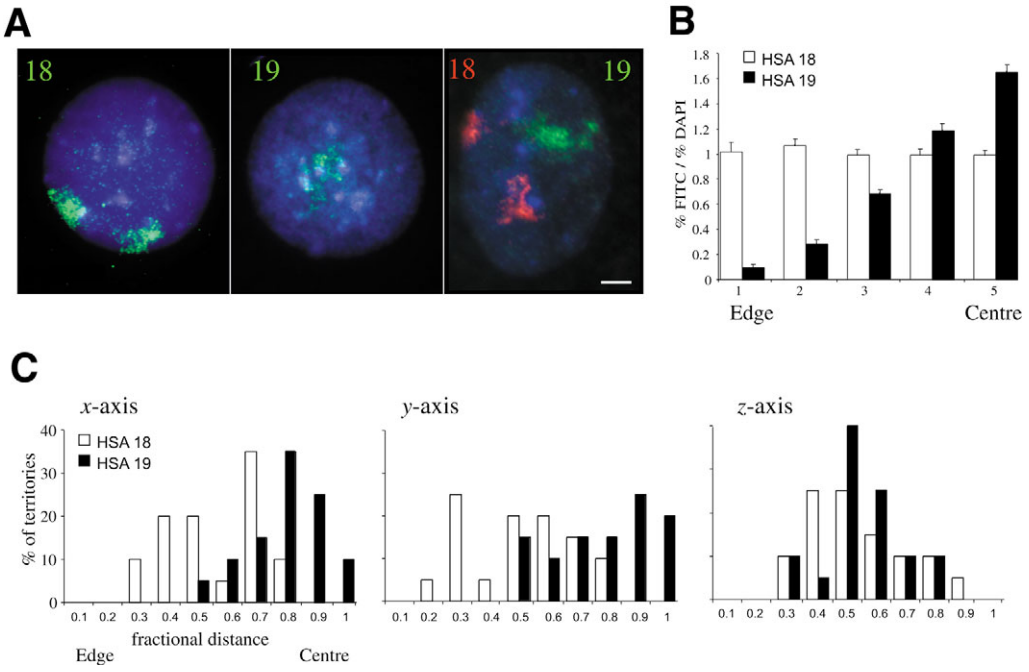

Fig. 1. The radial distribution of HSA18 and 19 in hES cells. (A) hES cell nuclei, counterstained with DAPI (blue) and hybridised with chromosome paints for HSA18 or 19. (B) Distribution of HSA18 and 19 hybridisation signals within the nucleus of H1 ES cells analysed by erosion of 2D images into five concentric shells from the edge (1) to the centre (5) of the nucleus. The mean (±s.e.m.) proportion of hybridisation signal, normalised to the amount of DAPI signal, is shown for each shell ($n=50$). (C) Analysis of HSA18 and 19 hybridisation signals within 3D-preserved hES cell nuclei. Graphs are the distributions of the centres of the HSA18 and 19 territories, along the fractional radius of each nucleus, along the x, y and z-axes ($n=20$). Bar, 5 μm.

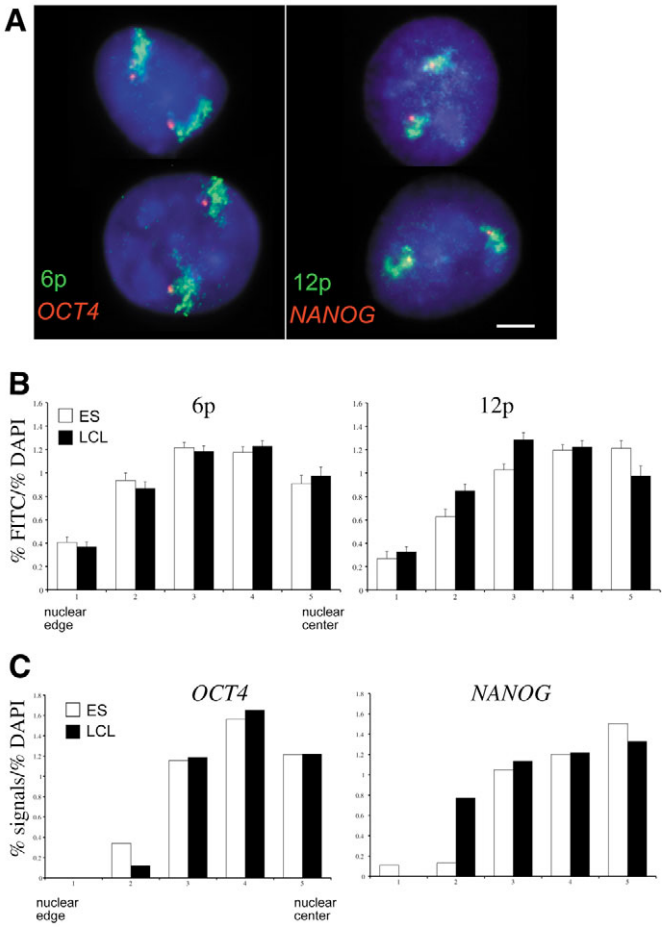

Fig. 2. Radial distribution of 6p, 12p, *OCT4* and *NANOG* in ES cells. (A) Interphase hybridisation of BAC probes containing *OCT4* or *NANOG* (red), and chromosome paints for either 6p or 12p (green), within the nuclei of human ES cells counterstained with DAPI (blue). (B) Distribution of HSA6p and 12p hybridisation signals within the nucleus of ES cells, by erosion of 2D images into 5 concentric shells from the edge (1) to the centre (5) of the nucleus. The mean (±s.e.m.) proportion of hybridisation signal, normalised to the amount of DAPI signal, is shown for each shell (n=50). C) Distribution of hybridisation signals from *OCT4* or *NANOG*-containing BACs within the nucleus of ES cells, by erosion of 2D images into five concentric shells from the edge (1) to the centre (5) of the nucleus. The proportion of hybridisation signals, normalised to the amount of DAPI signal, is shown for each shell (n=50). Bar, 5 μm.

As well as having a radial organisation within the nucleus, CTs also have a distinctive architecture themselves. In differentiated cells, gene-rich domains and regions of coordinately regulated gene expression, loop out from CTs (Volpi et al., 2000; Mahy et al., 2002a). One of the gene-rich domains of the human genome that we have previously shown to loop out from its CT in LCLs is the distal part of 11p15.5 (Mahy et al., 2002a). We found that loci from 11p15.5 (positions 0.25-2.1 Mb, NCBI build 35, http://www.ensembl.org/Homo_sapiens) are also located outside the 11p territory in hES cell nuclei, even though this region of the genome does not contain any genes with a known role in maintaining pluripotency (Table 1). In contrast, *RCN*, which is expressed in both LCLs (Mahy et al., 2002b) and hES cells (Ramalho-Santos et al., 2002), but which is located in a low gene-density region at 11p13 (32Mb), remains inside the CT (Table 1). Therefore, CT architecture is well developed in hES cells, and is organised in a similar manner to differentiated cells, with regions of generally high gene density located out side of CTs.

To determine whether a specific CT architecture could be detected at pluripotency genes expressed in ES cells, we analysed the intra-CT position of *NANOG* and *OCT4*. We measured the distances between hybridisation signals for BACs for the specific loci, and the visible edge of the hybridisation signal for the corresponding CT (Mahy et al., 2002). We found that *NANOG* is located well within the 12p CT in both LCL and ES cells (Table 1, Fig. 3A).

However, the intra-CT behaviour of *NANOG* contrasts with that of *OCT4*, which is a non-class I gene, embedded within the MHC Class I region (Fig. 3A). Classical class I region genes are expressed constitutively in human LCLs and fibroblasts. Unlike mES cells, hES cells also express class I genes (Tian et al., 1997; Drukker et al., 2002; Draper et al., 2002; Carpenter et al., 2004). The Class I and Class III regions have been found outside CTs in LCLs (Volpi et al., 2000). We confirmed this using BACs that flank *OCT4* and that contain either another non-class I gene (*FLOT1*), or the most centromeric genes of the class I region (*MICB*). We found that these regions were located, on average, outside the 6p CT in hES cells (Table 1 and Fig. 3A). However, the mean position of the intervening *OCT4* locus differed between ES and LCL cells. On average, *OCT4* was just inside the CT in LCLs, but outside the CT in ES cells (Table 1 and Fig. 3A). This difference was small, but statistically significant (P=0.041). Analysing the distribution of distances revealed that this

Table 1. Intra-CT position of loci in hES cells and LCLs

Locus	Cytogenetic position	Genomic position (Mb)	Probe name	Position relative to CT edge	
				LCL (μm)	ES (μm)
IFITM3	11p15.5	0.2	D11S483	–1.4±0.3	–0.70±1.13
INS	11p15.5	2.1	cINS/IGF2	–0.6±0.2	–0.55±0.15
RCN	11p13	32	cH11148	0.6±0.2	0.26±0.04
NANOG	12p13.31	7.8	RP11-358I17	0.23±0.06	0.32±0.04
FLOT1	6p21.33	30.8	RP11-324F19	–0.07±0.07	–0.11±0.08
OCT4	6p21.33	31.2	RP11-1058J10	0.03±0.06	–0.15±0.09
MICB	6p21.33	31.6	RP11-184F16	–0.25±0.09	–0.31±0.16

The cytogenetic position and genome position (from NCBI build 35, http://www.ensembl.org/Homo_sapiens) of each locus is indicated, together with the name of the cosmid or BAC probe used in FISH. Mean (±s.e.m.) position, in μm, of specific loci relative to the edge of CTs in nuclei from hES cells and from LCLs. Negative values indicate positions outside the visible limits of the CT. LCL data for 11p15.5 loci is taken from Mahy et al., 2002a.

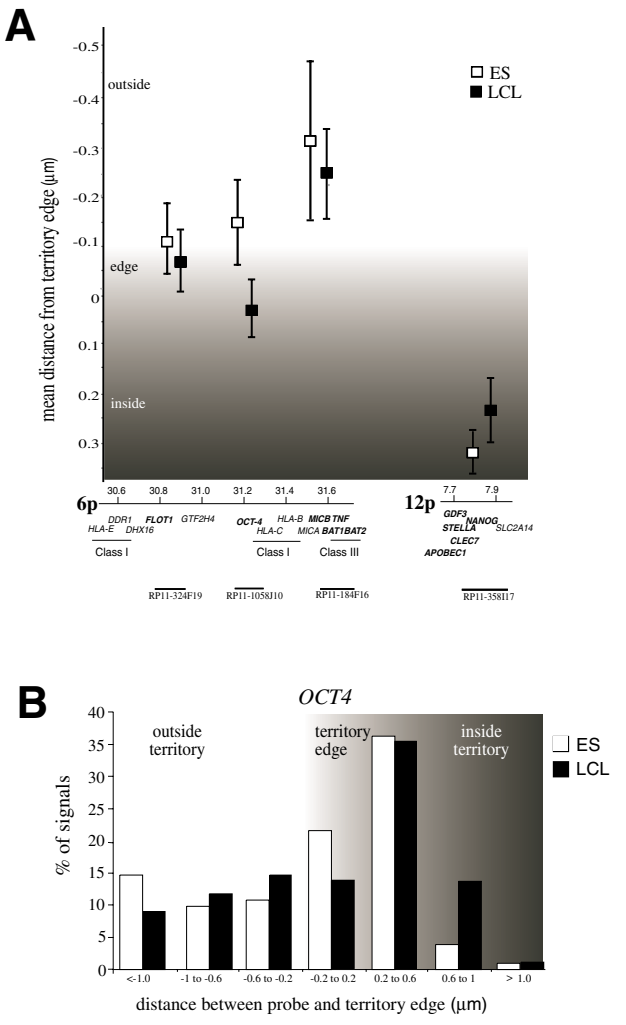

Fig. 3. Intrachromosome territory organisation of *NANOG* and *OCT4*. (A) Position (mean±s.e.m.) in μm, relative to the inside, edge or outside CTs, for loci including *NANOG* and *OCT4*, as well as loci flanking *OCT4*, in the nuclei of hES cells (□) and LCLs (■) (*n*=100). Negative values indicate localisation outside the CT. The map of the genomic regions around *OCT4* and *NANOG* (according to NCBI build 35) is shown below. Genes present in the BACs used are highlighted in bold. (B) Histogram of the distribution of FISH signals from a BAC containing *OCT4*, relative to the edge of the chromosome 6p CT, in nuclei from hES cells (open bars) and LCLs (filled bars). Negative distance indicates localisation outside the visible limits of the CT (*n*=100).

change in mean intra-CT position represented, not a change in the overall percentage of *OCT4* loci found well (>0.2 μm) outside the CT (36% for both LCLs and ES cells), but a reduction in the number of loci found deep within the CT (>0.6 μm), and a consequent increase in the *OCT4* loci positioned at the CT edge (Fig. 3B).

During the differentiation of mouse ES cells, the movement of loci relative to the surface of CTs is generally accompanied by cytologically detectable changes in chromatin condensation (Chambeyron and Bickmore, 2004). To investigate this further, we measured the interphase distance (*d*) between *OCT4* and the flanking BAC clones. In all cases, the distribution of *d* values conformed to that expected of a random-walk model of chromatin structure (s.d.=0.52-0.6; median/mean ~1.0) (Sachs et al., 1995; Chambeyron and Bickmore, 2004). There was no significant difference in the mean-squared interphase distance (<d^2>) between *OCT4* and *MICB* BACS (genomic distance, 350 kb) for hES cells and LCLs (<d^2>=0.5±0.06 and 0.41±0.04 μm^2 respectively, *P*=0.41). However, there was a significantly larger interphase separation between *OCT4* and *FLOT1* (genomic distance, 400 kb) in LCLs (<d^2>=0.33±0.04 μm^2) compared to hES cells (0.24±0.03 μm^2), *P*=0.04. In both LCLs and hES cells the large sizes of the d^2 values measured around *OCT4*, are consistent with the presence of a generally open chromatin fibre structure, rather than a compact one (Gilbert et al., 2004).

These data suggest that both the intra-CT architecture and the long-range chromatin configuration around the *OCT4* locus differ between hES cells and a differentiated cell type that does not express this marker of pluripotency.

Localisation and clustering of centromeres in human ES cells

We detected distinctive nuclear organisation of chromosome arms and specific gene loci in hES cells. To investigate other non-genic regions we compared the position and number of centromere clusters in hES cells with that in two diploid differentiated cell types: LCLs and primary fibroblasts. Centromeres were detected in paraformaldehyde-fixed cells using antibodies that recognise CENP-C or CREST serum. There were no significant differences in the extent of centromere clustering between hES cells and these two differentiated cell types. The average number of centromere signals scored per cell was 34, 36 and 38 for ES, LCL and proliferating fibroblasts, respectively (*n*=20). Centromere position was analysed with respect to the nuclear periphery, or to the nucleolus (detected with antibody that recognises pKi67) (Fig. 4A). A significantly lower proportion of centromeres was associated with the nuclear periphery of hES cells in comparison with LCLs (*P*<0.04) or fibroblasts (*P*<0.001) (Fig. 4B). Similar proportions of centromeres were associated with nucleoli in hES cells and fibroblasts (*P*>0.39). In hES cells a significantly higher proportion of centromeres were not associated with either the nuclear periphery or the nucleolus than either differentiated cell type (*P*<0.004). These differences were confirmed by examination of centromere distribution through the *z*-axis of nuclei (Fig. 4C). Centromeres have a normal distribution along the *z*-axis of ES cell nuclei, in contrast with a bimodal distribution towards the top and bottom surface of the nucleus of fibroblasts.

Telomeres are dispersed throughout the nucleoplasm of differentiated cells (Weierich et al., 2003). Most primary diploid somatic cells, including fibroblasts, do not have active telomerase activity, and so are subject to progressive telomere shortening. Germ cells and stem cells in contrast have active telomerase, and robust telomerase activity is detected in hES cells (Thomson et al., 1998). We found that telomeres had a near-normal distribution in the centre of the nucleus of both hES cells and LCLs, though this is skewed towards the bottom of the nucleus in fibroblasts (Fig. 4D).

Lastly, we also analysed the nuclear distribution of PML bodies. The function of these nuclear bodies remains unknown, though they have been implicated in transcriptional regulation, apoptosis, and DNA damage and stress sensing (Dellaire and

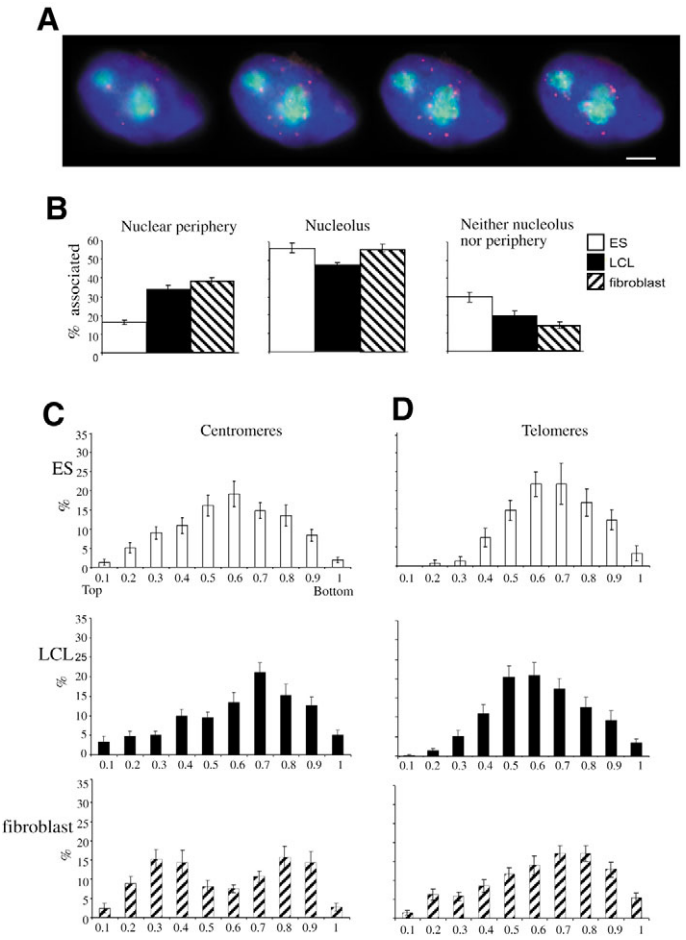

Fig. 4. Centromere and telomere localisation in hES cells. (A) Localisation of centromeres (CREST, red), and nucleoli (Ki67, green) in single image frames, taken at 0.75 μm intervals, through the *z*-axis of hES cell nuclei counterstained with DAPI (blue). Note the absence of centromeres from the nuclear periphery. (B) Mean (±s.e.m.) proportion of centromeres per cell that are associated with the nuclear periphery (left), the nucleolus (middle), or neither of these nuclear compartments (right), in H1 ES cells (open bars), LCLs (filled bars) and fibroblasts (hatched bars) (*n*=20). The mean (±s.e.m.) distribution of (C) centromeres and (D) telomeres through the *z*-plane from the top (0) to the bottom (1) of nuclei from ES, LCL and fibroblast cells (*n*=20). Bar, 5 μm.

Bazett-Jones, 2004). Their nuclear distribution has not been extensively studied, but many transcriptionally active genomic regions, including parts of the major histocompatibility complex (MHC) at 6p, are reported to be associated with them (Wang et al., 2004). The average number of PML bodies scored in hES cells (11), is lower than that seen in LCLs (15) or fibroblasts (27), but despite the differences in abundance of PML bodies between cell types, their intranuclear distribution towards the central mid-plane of the nucleus was the same in all three cell types (data not shown).

Discussion

The radial distribution of chromosome territories is present in hES cells

We found that a major organisational feature of human nuclei, the radial organisation of CTs, is already established in hES cells. Gene-poor chromosome 18 is located toward the nuclear periphery of ES cells, whereas gene-rich HSA19 is more internal (Fig. 1). HSA18 is seen towards the nuclear periphery of a variety of differentiated cell types including lymphocytes (Croft et al., 1999), keratinocytes, and leukaemic and cancer cell lines (Cremer et al., 2003). However, a peripheral localisation of HSA18 was not seen in the very flat nuclei of amniotic fluid cells and quiescent fibroblasts (Bridger et al., 2000; Cremer et al., 2001). The nuclei of H1 ES cells are quite spherical (average height:length ratio=1.02±0.1), more similar to the shape of lymphocyte nuclei (ratio=1.00±0.1), than to those of fibroblasts (ratio=0.25±0.4). A differential localisation of HSA18 and 19 was also reported for granulocyte-macrophage colony-forming cells (GM-CFCs) and it has been suggested that radial distribution is also present in the pluripotent haematopoietic progenitor cells (Cremer et al., 2003). As we show that this radial distribution is already present in hES cells, we think it highly likely that a similar nuclear organisation will be present in most, if not all, foetal and adult stem cells.

Chromosome 12p is located in the centre of the nucleus in ES cells

Differences in the radial distribution of mouse chromosomes have been documented in different tissues and during T-cell differentiation (Parada et al., 2004; Kim et al., 2004). However, to date no significant change in radial position of a human chromosome within the nucleus had been documented during differentiation, although there may be changes in chromosome associations (Kuroda et al., 2004).

Here we have detected a significantly more central nuclear localisation for the short arm of human chromosome 12 in ES cells. It is interesting to note that recurrent gains of chromosome 12, including iso12p, have been found in human ES cells (Draper et al., 2004). It has been suggested that increased dosage of genes on chromosome 12 (and therefore presumably increased gene expression levels) is advantageous to the propagation of undifferentiated ES cells. Although the functional significance of positioning in the nuclear centre of mammalian cells is unknown, the presence in this zone of the nucleus of the most gene-dense human chromosomes (Boyle et al., 2001) suggests that it may confer some transcriptional advantage. Chromosome 12p contains a cluster of genes whose expression is linked to the maintenance of pluripotency. *NANOG* expression is required to maintain ES cells in an undifferentiated state (Zaehres et al., 2005). It is located just proximal of two other genes, *STELLA* and *GDF3*, which are also expressed in ES cells and downregulated upon differentiation (Clark et al., 2004). A BAC that covers this gene cluster also shows a more central nuclear position in hES cells when compared with LCLs (Fig. 2C). Is it possible that it is the transcriptional activity of this gene cluster that is driving the nuclear localisation of 12p in hES cells?

Preferential association of inactive genes with the nuclear periphery has been reported in differentiated cells, compared with their position in expressing cell types (Zink et al., 2004). However, we detect no association of either *NANOG* or *OCT4* with the nuclear periphery in differentiated cells (Fig. 2C).

A relocalisation of *OCT4*, with respect to its chromosome territory, in hES cells

In contrast to the central nuclear localisation of 12p and *NANOG* in human ES cells, we detected no significant difference in the radial nuclear position of 6p or *OCT4* between ES and differentiated cells. Both gene and chromosome territory remain in an intermediate nuclear position (Fig. 2). However, we found that compared with LCLs, *OCT4* is located significantly closer to, or just beyond the CT edge in hES cells (Fig. 3). In both cell types, the flanking Class I and Class III MHC regions were located outside the 6p CT, consistent with other results (Volpi et al., 2000). The local chromatin structure of *OCT4* has not been studied in hES cells but, in the mouse, increased DNA methylation and histone deacetylation of the *Oct4* enhancer/promoter are seen in trophoblast cells compared with ES cells (Hattori et al., 2004). The data we have presented here would be consistent with a more long-range remodelling of chromatin architecture around *OCT4*, which might also contribute to its transcriptional regulation.

Therefore, for both of the best-studied genes involved in pluripotency, we find a distinctive nuclear organisation in human ES cells. In the case of *NANOG*, the whole chromosome arm is localised towards the nuclear centre, whereas for *OCT4* there is a more localised reorganisation that allows the gene to leave the confines of its chromosome territory.

Internal nuclear distribution of centromeres in hES cells

In most human cell types, the predominant reported distribution of centromeres is toward the nuclear periphery (reviewed by Gilchrist et al., 2004). In contrast, we have found that centromeres seem to be found mainly within the nuclear interior of hES cells (Fig. 4). Factors determining centromere position in the nucleus are not clear. Under some conditions, the levels of histone acetylation of centric heterochromatin can alter centromere position in human and mouse somatic cells (Taddei et al., 2001) and, in the mouse, histone hypoacetylation at satellite repeats only occurs upon the induction of differentiation of mES cells (Keohane et al., 1996). Histone modifications in hES cells have yet to be examined. Localisation of centromeres away from the nuclear periphery may also reflect the rapid cell cycles of hES cells. In turn the localisation of centromeres within the nucleus may influence mechanisms of gene silencing (Fisher and Merkenschlager, 2002). Most interestingly, changes in the nuclear distribution of centromeres have recently been correlated with the maturation and developmental competency of mouse oocytes (Zuccotti et al., 2005).

To our knowledge, this is the first study of nuclear organisation in human ES cells. We have found that hES cell nuclei have a distinct nuclear architecture, especially at loci involved in maintaining pluripotency. Understanding how this nuclear organisation is established and how it influences gene expression might subsequently allow a better understanding of pluripotency.

This work is dedicated to the memory of John Clark, who died 12th August 2004, and who is much missed. A.E.W. was funded by a stem cell studentship from the Medical Research Council, UK. W.A.B. is a Centennial fellow of the James S. McDonnell foundation. The work was supported in part by the EU FP6 Network of Excellence Epigenome (LSHG-CT-2004-503433). We thank W. Earnshaw (University of Edinburgh) for the gift of anti-CenpC antibody.

References

Alcobia, I., Quina, A. S., Neves, H., Clode, N. and Parreira, L. (2003). The spatial organization of centromeric heterochromatin during normal human lymphopoiesis: evidence for ontogenically determined spatial patterns. *Exp. Cell Res.* **290**, 358-369.

Beil, M., Durschmied, D., Paschke, S., Schreiner, B., Nolte, U., Bruel, A. and Irinopoulou, T. (2002). Spatial distribution patterns of interphase centromeres during retinoic acid-induced differentiation of promyelocytic leukemia cells. *Cytometry* **47**, 217-225.

Boyle, S., Gilchrist, S., Bridger, J. M., Mahy, N. L., Ellis, J. A. and Bickmore, W. A. (2001). The spatial organization of human chromosomes within the nuclei of normal and emerin-mutant cells. *Hum. Mol. Genet.* **10**, 211-219.

Bridger, J. M., Boyle, S., Kill, I. R. and Bickmore, W. A. (2000). Re-modelling of nuclear architecture in quiescent and senescent human fibroblasts. *Curr. Biol.* **10**, 149-152.

Carpenter, M. K., Rosler, E. S., Fisk, G. J., Brandenberger, R., Ares, X., Miura, T., Lucero, M. and Rao, M. S. (2004). Properties of four human embryonic stem cell lines maintained in a feeder-free culture system. *Dev. Dyn.* **229**, 243-258.

Carvalho, C., Pereira, H. M., Ferreira, J., Pina, C., Mendonca, D., Rosa, A. C. and Carmo-Fonseca, M. (2001). Chromosomal G-dark bands determine the spatial organization of centromeric heterochromatin in the nucleus. *Mol. Biol. Cell* **12**, 3563-3572.

Chambeyron, S. and Bickmore, W. A. (2004). Chromatin decondensation and nuclear reorganization of the HoxB locus upon induction of transcription. *Genes Dev.* **18**, 1119-1130.

Clark, A. T., Rodriguez, R. T., Bodnar, M. S., Abeyta, M. J., Cedars, M. I., Turek, P. J., Firpo, M. T. and Reijo Pera, R. A. (2004). Human STELLAR, NANOG, and GDF3 genes are expressed in pluripotent cells and map to chromosome 12p13, a hotspot for teratocarcinoma. *Stem Cells* **22**, 169-179.

Cremer, M., von Hase, J., Volm, T., Brero, A., Kreth, G., Walter, J., Fischer, C., Solovei, I., Cremer, C. and Cremer, T. (2001). Non-random radial higher-order chromatin arrangements in nuclei of diploid human cells. *Chromosome Res.* **9**, 541-567.

Cremer, M., Kupper, K., Wagler, B., Wizelman, L., von Hase, J., Weiland, Y., Kreja, L., Diebold, J., Speicher, M. R. and Cremer, T. (2003). Inheritance of gene density-related higher order chromatin arrangements in normal and tumor cell nuclei. *J. Cell Biol.* **162**, 809-820.

Croft, J. A., Bridger, J. M., Boyle, S., Perry, P., Teague, P. and Bickmore, W. A. (1999). Differences in the localization and morphology of chromosomes in the human nucleus. *J. Cell Biol.* **145**, 1119-1131.

Dellaire, G. and Bazett-Jones, D. P. (2004). PML nuclear bodies: dynamic sensors of DNA damage and cellular stress. *BioEssays,* **26**, 963-977.

Draper, J. S., Pigott, C., Thomson, J. A. and Andrews, P. W. (2002). Surface antigens of human embryonic stem cells: changes upon differentiation in culture. *J. Anat.* **200**, 249-258.

Draper, J. S., Smith, K., Gokhale, P., Moore, H. D., Maltby, E., Johnson, J., Meisner, L., Zwaka, T. P., Thomson, J. A. and Andrews, P. W. (2004). Recurrent gain of chromosomes 17q and 12 in cultured human embryonic stem cells. *Nat. Biotechnol.* **22**, 53-54.

Drukker, M., Katz, G., Urbach, A., Schuldiner, M., Markel, G., Itskovitz-Eldor, J., Reubinoff, B., Mandelboim, O. and Benvenisty, N. (2002). Characterization of the expression of MHC proteins in human embryonic stem cells. *Proc. Natl. Acad. Sci. USA* **99**, 9864-9869.

Fisher, A. G. and Merkenschlager, M. (2002). Gene silencing, cell fate and nuclear organisation. *Curr. Opin. Genet. Dev.* **12**, 193-197.

Gilbert, N., Boyle, S., Fiegler, H., Woodfine, K., Carter, N. P. and Bickmore, W. A. (2004). Chromatin architecture of the human genome: gene-rich domains are enriched in open chromatin fibers. *Cell* **118**, 555-566.

Gilchrist, S., Gilbert, N., Perry, P. and Bickmore, W. A. (2004). Nuclear organization of centromeric domains is not perturbed by inhibition of histone deacetylases. *Chromosome. Res.* **12**, 505-516.

Ginis, I., Luo, Y., Miura, T., Thies, S., Brandenberger, R., Gerecht-Nir, S., Amit, M., Hoke, A., Carpenter, M. K., Itskovitz-Eldor, J. et al. (2004). Differences between human and mouse embryonic stem cells. *Dev. Biol.* **269**, 360-380.

Hattori, N., Nishino, K., Ko, Y. G., Hattori, N., Ohgane, J., Tanaka, S. and Shiota, K. (2004). Epigenetic control of mouse Oct-4 gene expression in

embryonic stem cells and trophoblast stem cells. *J. Biol. Chem.* **279**, 17063-17069.

Keohane, A. M., O'Neill, L. P., Belyaev, N. D., Lavender, J. S. and Turner, B. M. (1996). X-Inactivation and histone H4 acetylation in embryonic stem cells. *Dev Biol*. **180**, 618-630.

Kim, S. H., McQueen, P. G., Lichtman, M. K., Shevach, E. M., Parada, L. A. and Misteli, T. (2004). Spatial genome organization during T-cell differentiation. *Cytogenet. Genome Res.* **105**, 292-301.

Kuroda, M., Tanabe, H., Yoshida, K., Oikawa, K., Saito, A., Kiyuna, T., Mizusawa, H. and Mukai, K. (2004). Alteration of chromosome positioning during adipocyte differentiation. *J. Cell Sci.* **117**, 5897-5903.

Mahy, N. L., Perry, P. E. and Bickmore, W. A. (2002a). Gene density and transcription influence the localization of chromatin outside of chromosome territories detectable by FISH. *J. Cell Biol.* **159**, 753-763.

Mahy, N. L., Perry, P. E., Gilchrist, S., Baldock, R. A. and Bickmore, W. A. (2002b). Spatial organization of active and inactive genes and noncoding DNA within chromosome territories. *J. Cell Biol.* **157**, 579-589.

Matin, M. M., Walsh, J. R., Gokhale, P. J., Draper, J. S., Bahrami, A. R., Morton, I., Moore, H. D. and Andrews, P. W. (2004). Specific knockdown of Oct4 and beta2-microglobulin expression by RNA interference in human embryonic stem cells and embryonic carcinoma cells. *Stem Cells* **22**, 659-668.

Parada, L. A., McQueen, P. G. and Misteli, T. (2004). Tissue-specific spatial organization of genomes. *Genome Biol.* **5**, R44.

Pera, M. F. and Trounson, A. O. (2004). Human embryonic stem cells: prospects for development. *Development* **131**, 5515-5525.

Ramalho-Santos, M., Yoon, S., Matsuzaki, Y., Mulligan, R. C. and Melton, D. A. (2002). "Stemness": transcriptional profiling of embryonic and adult stem cells. *Science* **298**, 597-600.

Sachs, R. K., van den Engh, G., Trask, B. and Hearst, J. E. (1995). A random-walk/giant-loop model for interphase chromosomes. *Proc. Natl. Acad. Sci. USA* **92**, 2710-2714.

Spector, D. L. (2003). The dynamics of chromosome organization and gene regulation. *Annu. Rev. Biochem.* **72**, 573-608.

Taddei, A., Maison, C., Roche, D. and Almouzni, G. (2001). Reversible disruption of pericentric heterochromatin and centromere function by inhibiting deacetylases. *Nat. Cell. Biol.* **3**, 114-120.

Tanabe, H., Muller, S., Neusser, M., von Hase, J., Calcagno, E., Cremer, M., Solovei, I., Cremer, C. and Cremer, T. (2002). Evolutionary conservation of chromosome territory arrangements in cell nuclei from higher primates. *Proc. Natl. Acad. Sci. USA* **99**, 4424-4429.

Thomson, J. A., Itskovitz-Eldor, J., Shapiro, S. S., Waknitz, M. A., Swiergiel, J. J., Marshall, V. S. and Jones, J. M. (1998). Embryonic stem cell lines derived from human blastocysts. *Science* **282**, 1145-1147.

Tian, L., Catt, J. W., O'Neill, C. and King, N. J. (1997). Expression of immunoglobulin superfamily cell adhesion molecules on murine embryonic stem cells. *Biol. Reprod.* **57**, 561-568.

Volpi, E. V., Chevret, E., Jones, T., Vatcheva, R., Williamson, J., Beck, S., Campbell, R. D., Goldsworthy, M., Powis, S. H., Ragoussis, J., Trowsdale, J. and Sheer, D. (2000). Large-scale chromatin organization of the major histocompatibility complex and other regions of human chromosome 6 and its response to interferon in interphase nuclei. *J. Cell Sci.* **113**, 1565-1576.

Wang, J., Shiels, C., Sasieni, P., Wu, P. J., Islam, S. A., Freemont, P. S. and Sheer, D. (2004). Promyelocytic leukemia nuclear bodies associate with transcriptionally active genomic regions. *J. Cell Biol.* **164**, 515-526.

Weierich, C., Brero, A., Stein, S., von Hase, J., Cremer, C., Cremer, T. and Solovei, I. (2003). Three-dimensional arrangements of centromeres and telomeres in nuclei of human and murine lymphocytes. *Chromosome Res.* **11**, 485-502.

Williams, R. R., Broad, S., Sheer, D. and Ragoussis, J. (2002). Subchromosomal positioning of the epidermal differentiation complex (EDC) in keratinocyte and lymphoblast interphase nuclei. *Exp. Cell Res.* **272**, 163-175.

Xu, C., Inokuma, M. S., Denham, J., Golds, K., Kundu, P., Gold, J. D. and Carpenter, M. K. (2001). Feeder-free growth of undifferentiated human embryonic stem cells. *Nat. Biotechnol.* **19**, 971-974.

Zaehres, H., Lensch, M. W., Daheron, L., Stewart, S. A., Itskovitz-Eldor, J. and Daley, G. Q. (2005). High-efficiency RNA interference in human embryonic stem cells. *Stem Cells* **23**, 299-305.

Zink, D., Amaral, M. D., Englmann, A., Lang, S., Clarke, L. A., Rudolph, C., Alt, F., Luther, K., Braz, C., Sadoni, N. et al. (2004). Transcription-dependent spatial arrangements of CFTR and adjacent genes in human cell nuclei. *J. Cell Biol.* **166**, 815-825.

Zuccotti, M., Garagna, S., Merico, V., Monti, M. and Redi, C. A. (2005). Chromatin organisation and nuclear architecture in growing mouse oocytes. *Mol. Cell. Endocrinol.* **234**, 11-17.